Frontiers in Scientific Research and Technology

Online ISSN: 2682-2970
Print ISSN: 2682-2962
http://fsrt.journals.ekb.eg

FSRT J 10 (2024) 31 – 40 10.21608/fsrt.2024.324450.1139

Determination of subsurface lineaments of the Paracel islands by the modern methods

To-Nhu Thi Ngo[1,2], Tho Huu Nguyen[1,2], Dat Viet Nguyen[2], Quynh Thanh Vo[2], Ahmed M. Eldosouky[3,*]

[1] Geophysical Division, General Department of Geology and Minerals, Hanoi, Vietnam

[2] University of Science, Vietnam National University, Hanoi, Vietnam

[3] Geology Department, Faculty of Science, Suez University, Suez, 43221, Egypt

ARTICLE INFO

Article history:
Submitted 28 September 2024
Received in revised form 6 November 2024
Accepted 13 November 2024

Keywords
Gravity,
EIGEN6C4,
Paracel islands.

ABSTRACT

In recent years, the global gravity model EIGEN-6C4 has been evaluated as one of the modern global gravity models with high resolution and accuracy thanks to the combination of satellite and ground data. This study uses different technical maps of Bouguer gravity anomaly data of the north of the Paracel Islands to contribute to a better understanding of the geological structure and tectonic faults. The modern edge detection techniques were tested on a synthetic model before being applied to the gravity data of the Paracel islands. The obtained structural map from the real model aligns with the primary fault system of the study area, which extends in multiple directions including NE–SW, NW–SE, WSW-ENE, WNW-ESE, and NNW-SSE. These orientations often represent the distribution and orientation of islands, reefs, and coral atolls; playing an important role in elucidating the geological structure of the study area and providing useful information about the study area's rich resources.

1. Introduction

The boundary detection methods are important in analyzing and processing magnetic and gravity data, especially in identifying subsurface structures such as faults, geological boundaries, and density or magnetic anomalies (Kafadar 2017; Saada et al., 2021, 2022; Ghomsi et al., 2022a,b; Sahoo et al., 2022a, b; Hamimi et al., 2023; Ekwok et al., 2024; Pham et al., 2024a). Some classical edge detection methods include the total horizontal derivative (THD), analytic signal (AS), tilt angle (TA), and vertical and horizontal derivatives (Ekinci et al., 2013). However, these methods may encounter issues, such as difficulty detecting edges at different positions simultaneously, or producing structure maps with low resolution (Eldosouky et al., 2022a, b; Kamto et al., 2023). Some authors have been introduced the balanced methods to outline the edges of deep structures more clearly (Pham et al., 2024b). One of the balanced techniques proposed by Wijns et al., (2005) is the theta map method (TM).

This method relies on the amplitude of the analytic signal to normalize the total horizontal gradient. The horizontal tilt angle method (TDX) introduced by Copper and Cowan (2006) uses the absolute value of the vertical derivative to normalize the total horizontal gradient.

Ferreira et al., (2013) suggested a method that uses the total horizontal gradient of THD to normalize the vertical derivative of THD called the tilt angle of THD method (ETHD). The improved horizontal tilt method (ITDX) proposed by Ma et al., (2016) uses higher-order derivatives to improve the boundary determination results. Chen et al., (2017) presented an advanced high-resolution technique called the improved theta map method (ITM). Pham et al., (2018) proposed the logistic method (L) based on the logistic function and the ratio of derivatives of AS. The logistic of the total horizontal gradient (LTHG) method is based on the ratio between the derivatives of the THD and the logistic function. The enhanced horizontal gradient amplitude (EHGA) and the improved logistic (IL) methods were suggested by Pham et al. (2020a, b). The EHGA technique uses the arcsine function of THD to improve resolution. The IL technique used the ratio of THD derivatives instead of AS derivatives.

An improved version of LTHG, based on the combination of the logistic function and the derivatives of the total horizontal gradient of the vertical derivative, is presented by Melouah and Pham (2021), known as the ILTHD method. In addition, many other boundary description methods have been developed to overcome the limitations of traditional methods and at the same time contribute to perfecting geological structure maps (Nasuti Y and Nasuti A, 2018; Nasuti et al., 2019; Oksum et al., 2021; Kafadar, 2022; Prasad et al., 2022a, b, c; Alvandi and Ardestani, 2023; Alvandi et al., 2023; Pham 2023, 2024a, b, c, d; Ai et al., 2024).

* Corresponding author at Suez University

E-mail addresses: dr_a.eldosoky@yahoo.com (Ahmed M. Eldosouky)

The Paracel Islands are a collection of islands, reefs, and coral atolls in the East Vietnam Sea (EVS). The formation of the Paracel Islands is the result of the combination of tectonic plate activity and coral reef development and is closely linked to the evolution process of the EVS. Fig. 1(a) illustrates the place of study region with a longitude extending from 110° E to 114° E and a latitude extending from 15° N and 18° N. This area is mainly between the South China Plate and the EVS Plate. These two plates play a major role in the formation and activity of the region's geology (Manh and Dinh, 2014). The Paracel Islands have great potential for oil, gas, and minerals under the seabed, especially oil and gas, along with minerals such as manganese and rare earths (Nhu et al., 2014). However, large-scale exploitation activities have not yet occurred due to the complex geological conditions of the region (Yang et al., 2022; Li et al., 2023). Elucidating the geological structures of the Paracel area contributes to predicting future exploration activities, and effectively protecting and developing the area.

In this study, we applied several modern boundary determination methods including ETHD, ITDX, ITM, EHGA, IL, and ILTHD to gravity data from the global gravity model EIGEN6C4 to elucidate the structural features of the Paracel islands. We evaluated the effectiveness of the methods on the synthetic model before interpreting real data of the Paracel Islands.

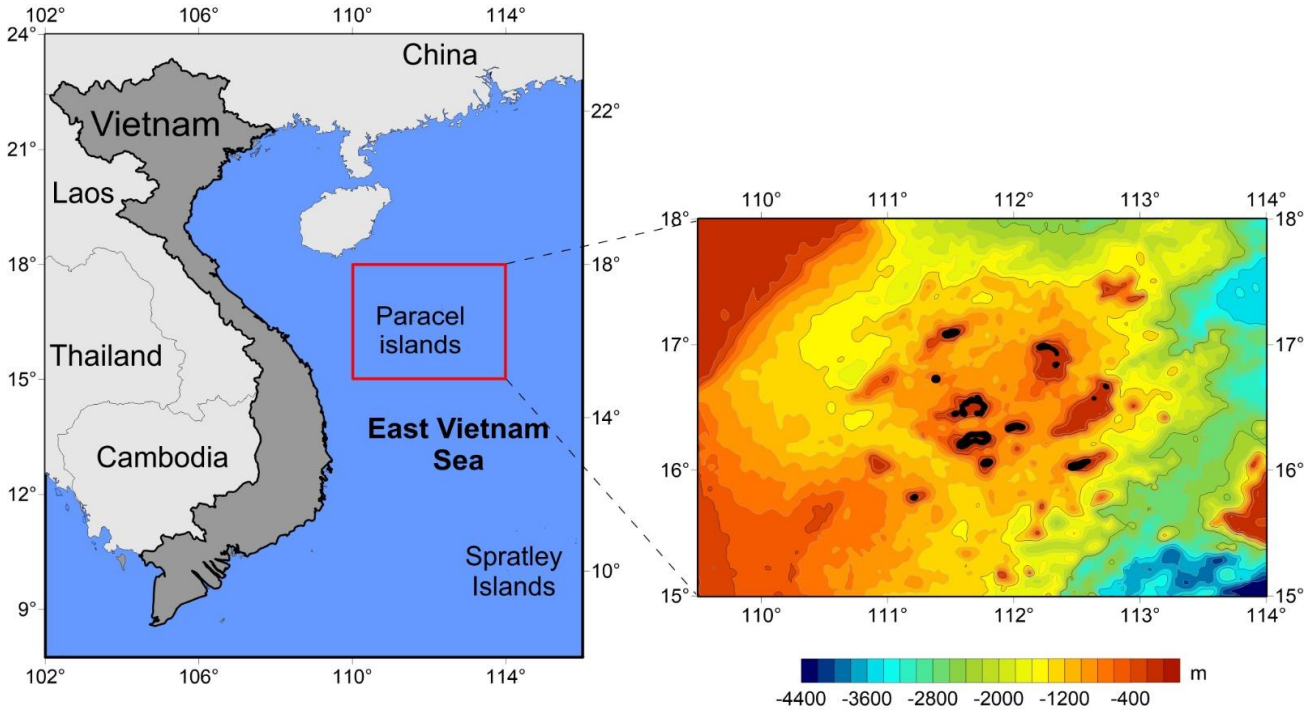

Fig. 1. (a) Location of the study area, **(b)** Bathymetry map. Paracel islands are shown by small black areas.

2. Geological context

The EVS is located east of the Indochinese Peninsula, south of China, east and south of Vietnam, as part of the western Pacific Ocean. The EVS is situated at the intersection of three major tectonic plates: Australian, Indian, and Eurasian plates (Luong et al.,2021). The EVS includes several small basins: Northwestern, Eastern, and Southwestern (Pham et al., 2022a). The EVS has a complex tectonic history, involving seafloor spreading, volcanic activity, and subsidence (Sibuet et al., 2016). These processes have contributed to the geological foundation on which the coral reefs and the Paracel Islands developed.

The Paracel Islands position is the northwest quadrant of the EVS. They lie to the southeast of Hainan Island (China) and east of the central coast of Vietnam. The Paracel Islands are a collection of islands, reefs, and coral atolls. The bathymetry map of the study area is presented in Fig. 1(b). The tectonic map of the region is depicted in Fig. 2(a). The process of seafloor spreading in the EVS, particularly in the northwest sub-basin, has led to the formation of deep basins. Plate tectonic movements have created fault systems and structural (fold and stratigraphic) traps are ideal for hydrocarbon accumulation. In addition, the development of coral reefs and limestone in the Paracel Islands not only formed coral islands but also provided a source for thick carbonate sediments. Large amounts of methane hydrates are predicted to accumulate in the Paracel Islands, indicating that it will become one of the significant carbon sinks in the world (Bouchat, 2014).

3. Data

Recently, applying of the edge filters to satellite data have shown great success in mapping geological structures (Sahoo and Pal, 2019; Sahoo et al., 2022a, b; Nzeuga et al., 2022; Ghomsi et al., 2022; Pham and Prasad, 2023, 2024).

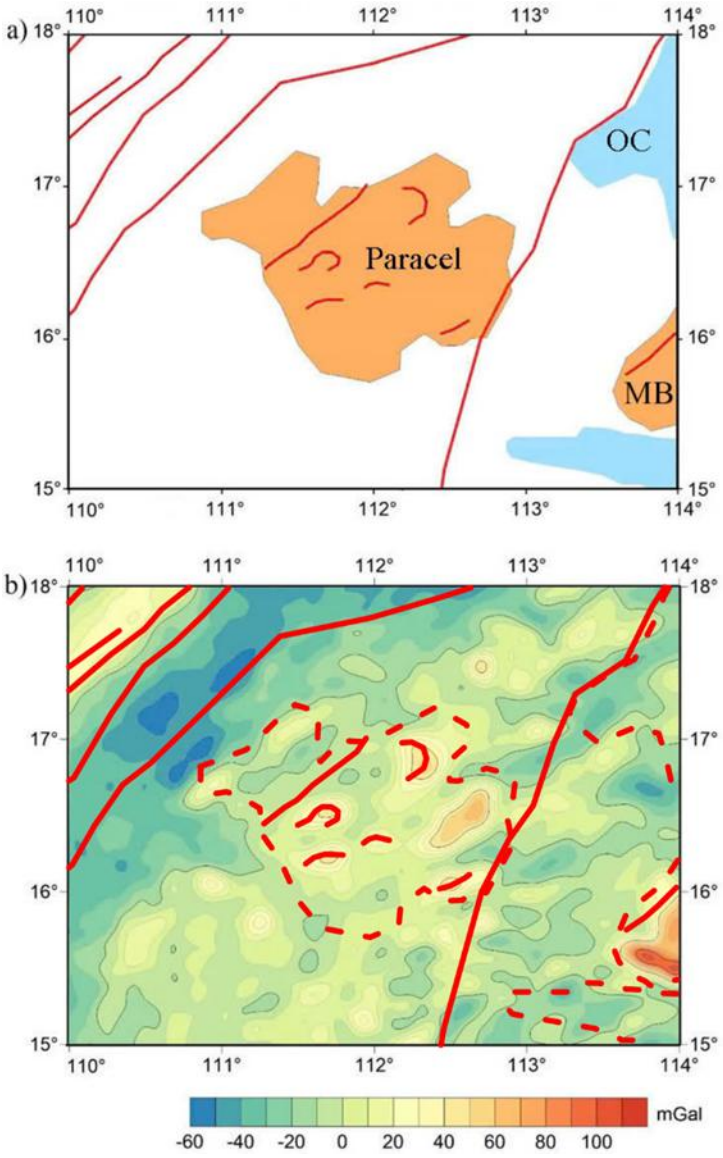

Fig. 2. (a) Tectonic map: OC: Oceanic crust, MB: Macclesfield Bank., **(b)** Free-Air gravity data of the Paracel Islands area. The red lines show the known faults, while the dashed red lines show the tectonic boundaries.

In this study, we used gravity data from the EIGEN6C4 model for detecting subsurface structures the study area. Figure 2b depicts the Free-air gravity dataset of the Paracel Islands provided by the EIGEN6C4 model. The EIGEN6C4 global gravity field model provides global coverage at a spatial resolution of about 12 km, which combines satellite data with surface gravity measurements such as LAGEOS, GRACE, GOCE, and DTU10 (Förste et al., 2014). The accuracy of the EIGEN-6C4 model has been confirmed by many articles, especially in the Vietnam area. Compared with EGM2008, GECO, SGG-UGM-1, SGG-UGM-2, XGM2019e_2159, and GGMPlus and concluded that the EIGEN6C4 model is one of the good EGM2008-related models when it shows more homogeneous accuracy over Vietnam (Pham et al., 2023). Some studies have used the EIGEN-6C4 model to map geological structures (Pal et al., 2016; Steffen et al., 2017; Roy et al., 2017; Melouah et al., 2023). Figure 6a illustrates the Bouguer gravity anomaly of the study area with the east containing high amplitude signals. The EIGEN-6C4 gravity model has been widely used and highly successful in interpreting structure lineament.

4. Methods

The ETHD method (Ferreira et al., 2013) is an enhanced version of the total horizontal derivative (THD) and can improve the ability to balance the anomalies of different amplitudes. The ETHD function is expressed as:

$$\mathrm{ETHD} = \operatorname{atan}\left(\frac{\frac{\partial \mathrm{THD}}{\partial z}}{\sqrt{\left(\frac{\partial \mathrm{THD}}{\partial x}\right)^2 + \left(\frac{\partial \mathrm{THD}}{\partial y}\right)^2}}\right), \quad (1)$$

with THD is defined as:

$$\mathrm{THD} = \sqrt{\left(\frac{\partial F}{\partial x}\right)^2 + \left(\frac{\partial F}{\partial y}\right)^2}. \quad (2)$$

Ma et al. (2016) introduced the improved horizontal tilt angle method (ITDX) that detects clearer geological boundaries based on a higher-order derivatives ratio. The ITDX method is given by:

$$\mathrm{ITDX} = \operatorname{atan}\frac{\sqrt{\left(\frac{\partial^2 F}{\partial z\,\partial x}\right)^2 + \left(\frac{\partial^2 F}{\partial z\,\partial y}\right)^2}}{\left|\frac{\partial^2 f}{\partial z\,\partial z}\right|}. \quad (3)$$

Chen et al. (2017) introduced a high-resolution method capable of detecting clearer subsurface structures known as the improved theta map method (ITM). The ITM method is calculated using the following formula:

$$\mathrm{ITM} = acos\frac{\sqrt{\left(\frac{\partial^2 f}{\partial z\,\partial x}\right)^2 + \left(\frac{\partial^2 f}{\partial z\,\partial y}\right)^2}}{\sqrt{\left(\frac{\partial^2 f}{\partial z\,\partial x}\right)^2 + \left(\frac{\partial^2 f}{\partial z\,\partial y}\right)^2 + \left(\frac{\partial^2 f}{\partial z\,\partial z}\right)^2}} \quad (4)$$

The EHGA method is an improved boundary determination technique by Pham et al., (2020a) using the arcsine function of the ratio between the vertical derivative and the total horizontal gradient of the THD. The formula for the EHGA filter is:

$$EHGA = \mathcal{R}\left(\operatorname{asin}\left(k\left(\frac{\frac{\partial THD}{\partial z}}{\sqrt{\left(\frac{\partial THD}{\partial x}\right)^2+\left(\frac{\partial THD}{\partial y}\right)^2+\left(\frac{\partial THD}{\partial z}\right)^2}}-1\right)+1\right)\right), \quad (5)$$

where $\mathcal{R}$ is the real part, and $k \geq 2$ will provide the best result.

Pham (2020b) proposed another boundary determination method, the improved logistic function to enhance the resolution of subsurface structures. The IL method uses the formula:

$$IL = \frac{1}{1+\exp[-p(R_{THD}-1)+1]}, \quad (6)$$

where $p = [2;5]$ will give high resolution results, and R_{THG} is defined by:

$$R_{THD} = \frac{\frac{\partial THD}{\partial z}}{\sqrt{\left(\frac{\partial THD}{\partial x}\right)^2+\left(\frac{\partial THD}{\partial y}\right)^2}} \quad (7)$$

The improved logistic total horizontal derivative (ILTHD) was suggested by Melouah and Pham (2021). The method is defined by the formula:

$$ILTHD = \left[1+\exp\left(-\frac{\frac{\partial ITHD}{\partial z}}{\sqrt{\left(\frac{\partial ITHD}{\partial x}\right)^2+\left(\frac{\partial ITHD}{\partial y}\right)^2}}\right)\right]^{-\alpha}, \quad (8)$$

with LTHD is calculated by:

$$ITHD = \sqrt{\left(\frac{\partial VD}{\partial x}\right)^2+\left(\frac{\partial VD}{\partial y}\right)^2} \quad (9)$$

where VD is the vertical derivative of the potential field F.

5. Results

In this section, we evaluate the effectiveness of modern edge detection methods (ETHD, ITDX, ITM, EHGA, IL, and ILTHD) through a synthetic gravity model (normal gravity field and gravity field with noise after upward continuation of 2km). This model consists of 5 objects, of which 3 prisms have the same size but different depths (A, B, C), and 2 thin prisms have various sizes and depths (D, E). The aim was to evaluate the ability of the methods to balance signals at different depths. Figure 3 (a, and b) illustrates 3D and plan views of the model. Table 1 details the parameters of the objects. Figure 3(c) shows gravity anomalies caused by prisms. Figure 4(a) presents the obtained edges from the ETHD, ITDX, and ITM methods in Fig. 3c. The ETHD, ITDX, and ITM methods can simultaneously balance anomalies of different amplitudes but they do not provide sharp signals on the boundaries of objects. The edges obtained from the ETHD method are thick and tend to overflow inside the object, making the obtained object size smaller than the real. The ITDX and ITM methods generate secondary edges surrounding objects at the deep source (B, C) and fail to accurately reflect the size of the thin prism (D). Figure 4(d) depicts the results obtained from the EHGA method with $k = 3$. The EHGA technique provided better results than the above methods in accurately representing the boundaries of objects. This method not only effectively balances anomalies at different depths but also yields clear and sharp results. The boundaries obtained from using the IL method $p = 2$ are displayed in Fig. 4e. Like the EHGA, the IL function balances the signals from different sources. Furthermore, the IL method provides higher resolution than the EHGA method. The boundaries of deep objects (B, D) obtained by the EHGA method are thicker than those by the IL method. The results obtained from the ILTHD method with $\alpha = 5$ are illustrated in Figure 4(f). We can observe that the ILTHD method offers the highest resolution among the above-discussed methods. However, the ILTHD method produces false edges around the objects (A, B, C).

Table 1. The parameter of the synthetic model.

Parameters / Prims	A	B	C	D	E
X-coordinates of the center (km)	50	50	50	125	175
Y-coordinates of the center (km)	200	125	50	125	125
Width (km)	70	70	70	5	15
Length (km)	45	45	45	200	200
Depth of top (km)	5	9	13	4	3
Depth of bottom (km)	9	13	17	6	5
Density contrast (g/cm^3)	0.1	-0.3	0.4	-0.5	0.2

We further evaluate the sensitivity of the above methods to noise. We added 10% Gaussian noise to the gravity anomaly. In this case, to reduce the influence of noise on the methods, we use an upward continuation to 2 km before applying the boundary determination methods (Nasuti and Nasuti, 2018; Pham et al., 2022b). The boundary map obtained from the ETHD method is depicted in Figure 5(a). This method can accurately determine the position of objects without creating secondary edges. However, the resulting edges are not clear and sharp. Besides, this method reflects the wrong size of objects even when the objects are shallow (D, E). Fig. 5(b), and 5(c) illustrate the structures obtained by ITDX and ITM methods. We can see that both methods are strongly affected by noise. The analysis maps obtained by these two methods have low resolution. Furthermore, ITDX and ITM methods generate false edges around the objects. The edges obtained by the EHGA and IL methods are shown in Fig. 5(d) and 5(e). Similar to the first case, the EHGA and IL methods can simultaneously balance large and small amplitude anomalies without creating false boundaries. The IL method provides higher resolution results than the ETHD, ITDX, ITM, and EHGA methods. The results obtained from the ILTHD method are presented in Fig. 5(f). We can see that the ILTHD technique is also strongly affected by noise. The boundaries of objects at deep sources (A, B, C) are faintly outlined and have low resolution.

The Bouguer gravity map from the EIGEN6C4 gravity model of the Paracel Islands is depicted in Figure 6a. To reduce the effects of noise, the gravity field was upward-continued to 2 km before using the methods (Fig 6b). The structural maps obtained from ETHD, ITDX, and ITM techniques are shown in Figures 7(a), 7(b), and 7(c). These methods highlight major boundaries and provide important information in identifying regional faults. However, the boundaries derived from the ITDX and ITM methods are interconnected, complicating mapping geological structures. Figures 7(d) and 7(e) show the geological structures calculated from the EHGA and IL methods. Both methods provide a large amount of information about the structures of the Paracel Islands. Furthermore, EHGA and IL can accurately delineate boundaries at shallow and deep sources without creating false boundaries. Like the results calculated from the synthetic model, the IL method also provides a higher-resolution geological structure map of the study area than the EHGA method. The structural geological of the Paracel Islands obtained from the ILTHD technique is depicted in Figure 7(f). Although the ILTHD technique can provide high-resolution results, it produces discrete boundaries in the analysis map. This method generates many false boundaries around known geological structures. These limitations make it difficult to assess the structural geology of the area.

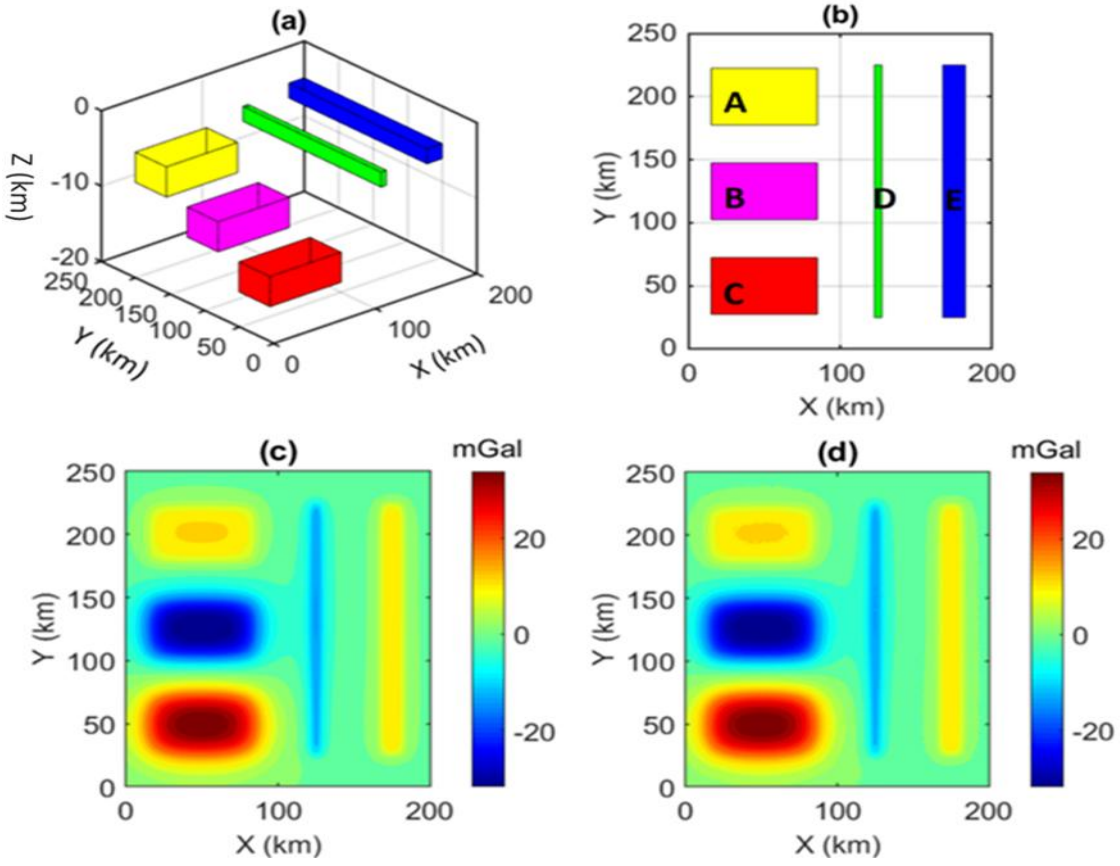

Fig. 3. (a) 3D, **(b)** 2D of the model, **(c)** gravity anomaly, **(d)** gravity anomaly with noise after upward continuation of 2 km.

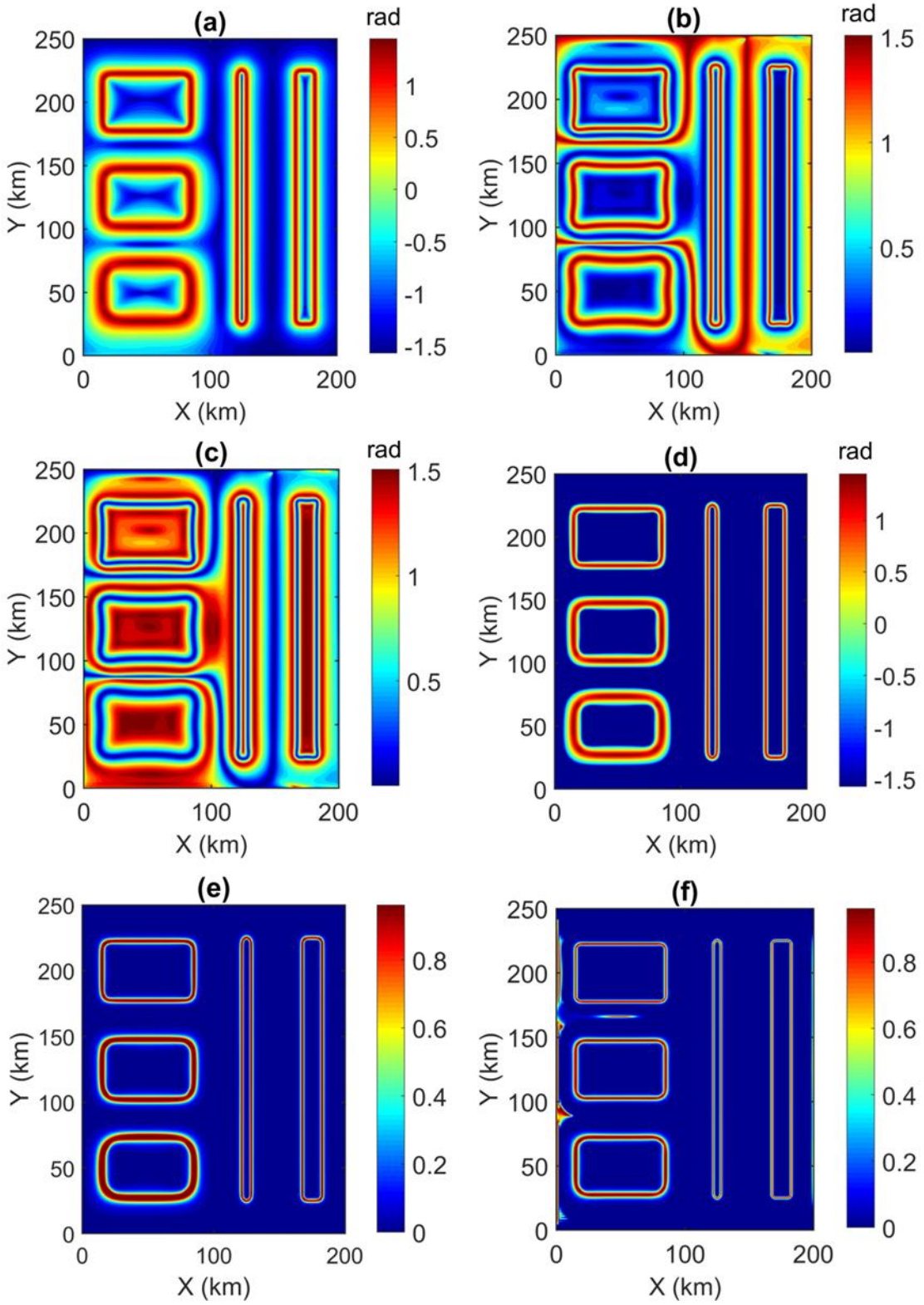

Fig. 4. The obtained results of gravity anomaly: **(a)** ETHD, **(b)** ITDX, **(c)** ITM, **(d)** EHGA, **(e)** IL, and **(f)** ILTHD.

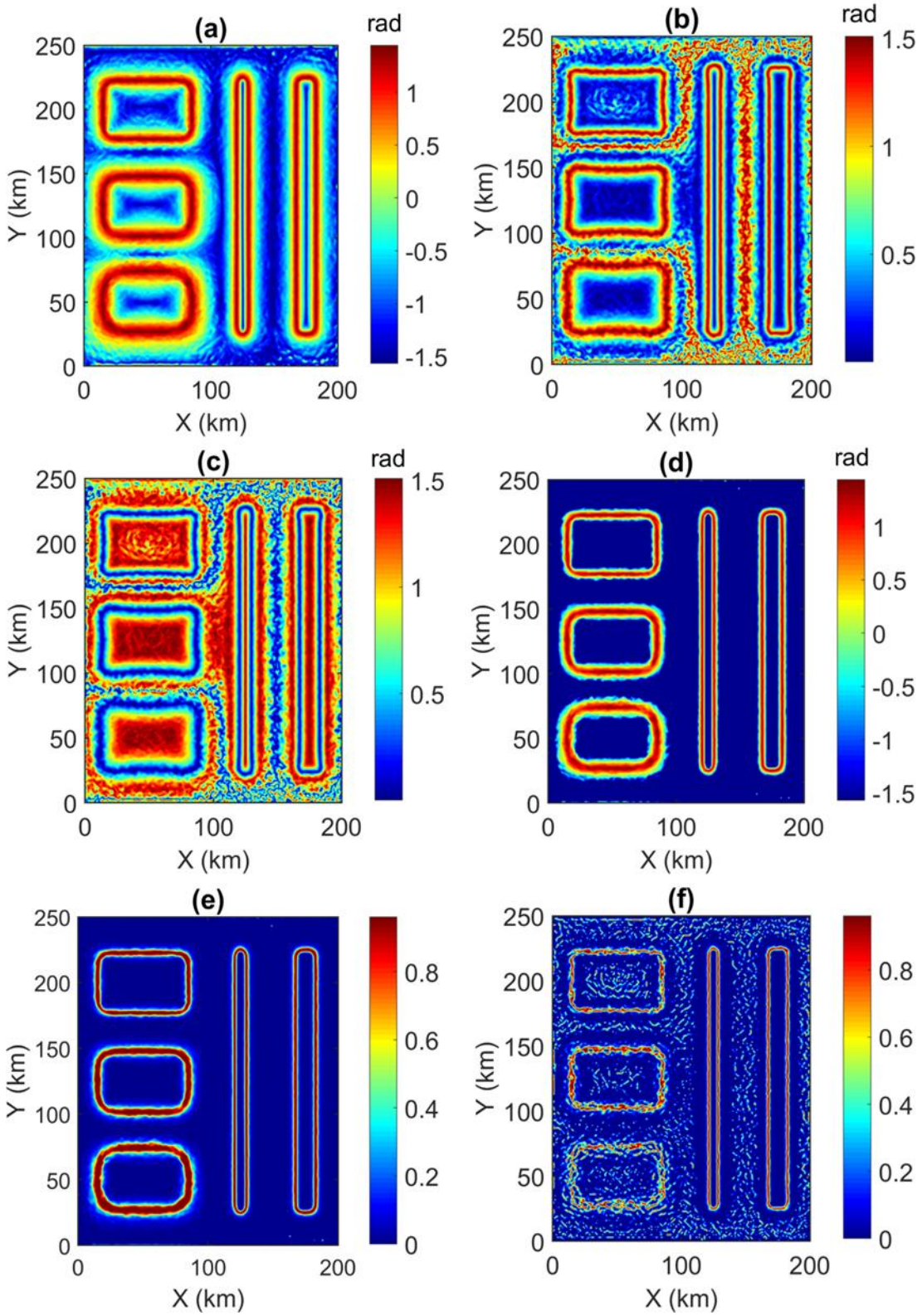

Fig. 5. The obtained results of gravity anomaly with noise after upward continuation of 2km: **(a)** ETHD, **(b)** ITDX, **(c)** ITM, **(d)** EHGA, **(e)** IL, and **(f)** ILTHD.

To improve the structural knowledge of the Paracel Islands, the EHGA, and IL methods were also applied to bathymetric data of the region. Although edge filters have been developed to interpret potential data, they were also used for interpreting non-potential fields (Beamish, 2012). Fig. 8(a), and 8(b) illustrate the maps obtained by applying the EHGA, and IL techniques to bathymetric data in Figure 1(b), respectively. Both methods provide a uniform gain for all transformed data and represent the signatures of topography due to depth variations.

6. Discussion

The ETHD, ITDX, and ITM methods can simultaneously balance gravity anomalies with large and small amplitudes. However, all three methods provided low-resolution images. The boundaries obtained from the ITDX and ITM methods are diffuse and interconnected. The EHGA and IL methods provided clear, sharp structures without creating false edges. The IL filter has a higher resolution than the EHGA filter. The ILTHD also generates high-resolution images but it is strongly affected by noise. The edges obtained using the real data appear quite discrete. The method also creates numerous false edges around known sources, complicating the classification of geological structures during real studies. It can be seen that both EHGA and IL methods are highly effective in determining the boundary. Therefore, we have combined these two methods to draw gravity and topographic lineaments of the Paracel islands. Figure 9 (a) illustrates the structure lineaments from the EHGA and IL methods (Fig. 7d and 7e). Figure 9 (b) describes the obtained topographic lines from the topographic EHGA and IL maps (Fig. 8). The gravity, topographic, and tectonic maps are overlapped, as depicted in Figure 10. Many structural lines correspond to topographic lineaments that may relate to young faults. Some gravity lineaments compare favorably with the signatures of topography.

The detection structure lineaments in the Paracel islands follow several directions, primarily NE–SW, NW–SE, NNW–SSE, WNW–ESE, and WSW–ENE. These orientations reflect the dominant structural and tectonic features, often associated with fault systems and geological formations in the EVS. Some obtained faults using EHGA and IL filters in the NE-SW and NW-SE directions (Fig.10) correspond to the existing faults. Due to the collision between the Indian and Eurasian plates, the northeast-oriented boundaries in the Paracel Islands area may be related to tectonic activity and movements of continental plates, especially the movement of the Shenhu plate (Pham et al., 2022a). The collision between these plates also created numerous NE-SW, NW–SE và WSW–ENE-oriented faults, reflecting the stress and displacement of the rock masses. The WNW–ESE direction could be influenced by forces from the west, where there is interaction between the Philippine Sea Plate and the Euro-Asian Plate. The NNW–SSE direction may relate to faults caused by the influence of the Sunda Plate or sliding between other plates. These orientations reflect the complexity of tectonic activities in the region, illustrating the continuous interaction and transformation between tectonic plates, which affects the geological structure and shape of the Paracel Islands.

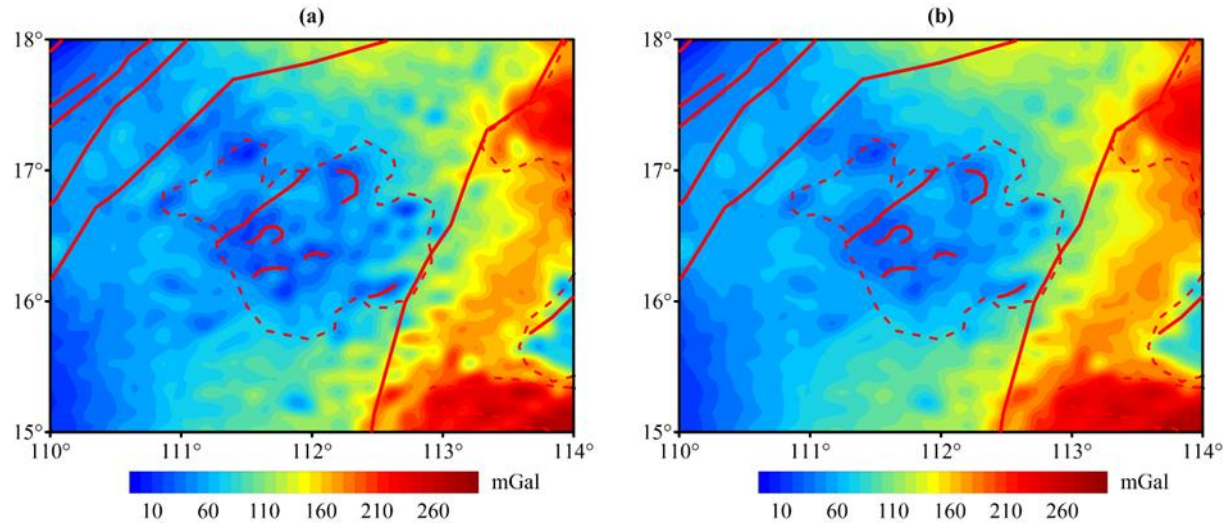

Fig. 6. (a) Bouguer gravity data, and **(b)** Bouguer gravity data after upward continuation of 2km of the Paracel islands area. The red lines show the known faults, while the dashed red lines show the tectonic boundaries.

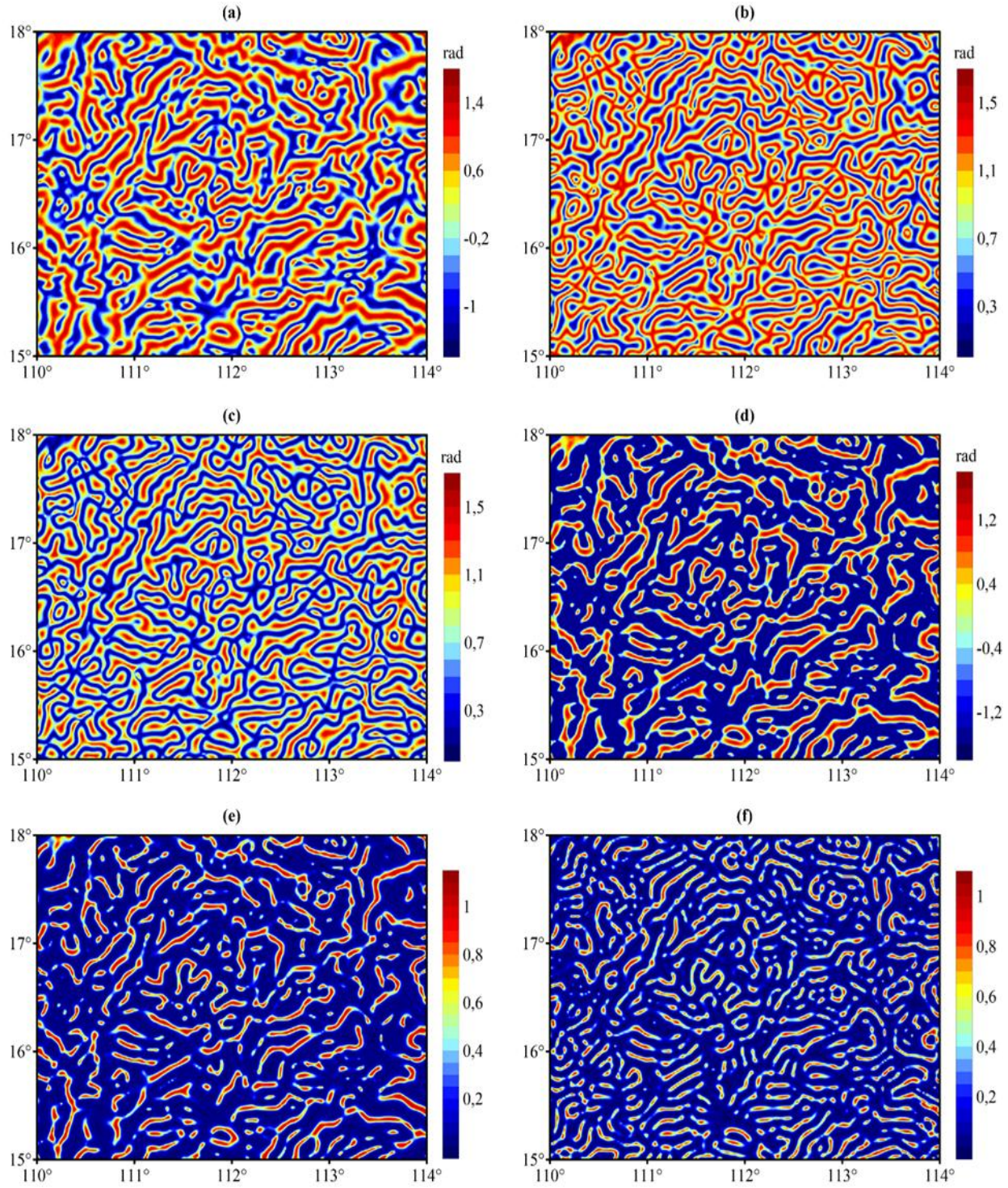

Fig. 7. The results of Bouguer gravity anomaly after upward-continued of 2km: **(a)** ETHD, **(b)** ITDX, **(c)** ITM, **(d)** EHGA, **(e)** IL, **(f)** ILTHD.

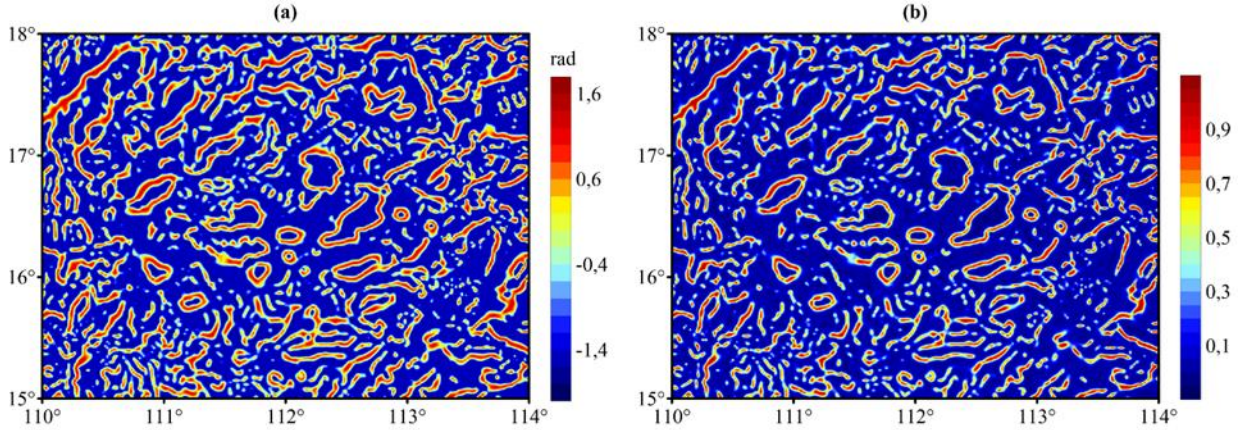

Fig. 8. The results of bathymetric data: **(a)** EHGA, **(b)** IL.

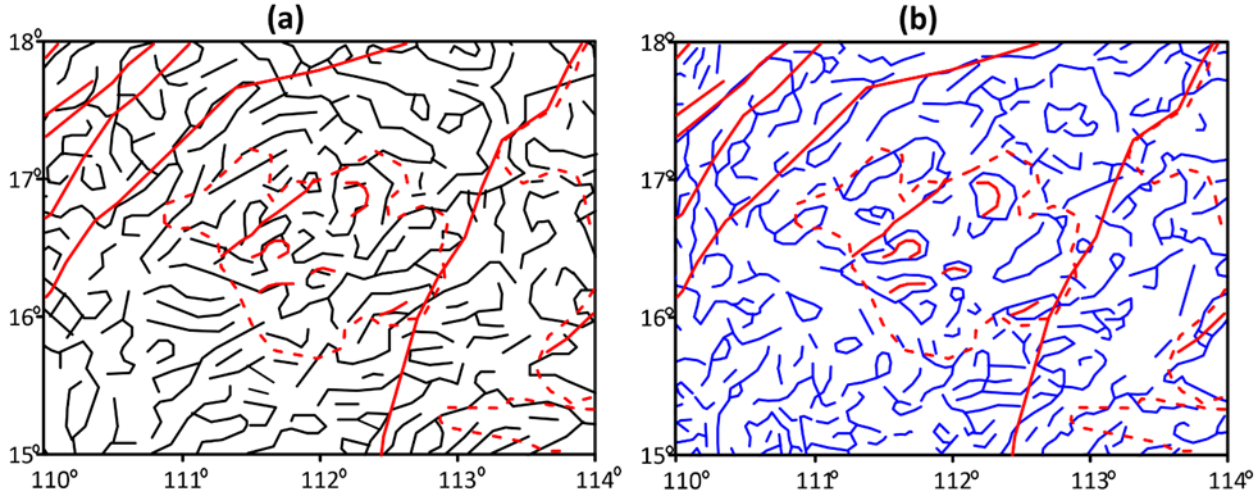

Fig. 9. (a) Gravity lineaments (black lines) and **(b)** Topographic lineaments (blue lines) by the EHGA and IL maps. The red lines show the known faults, while the dashed red lines show the tectonic boundaries.

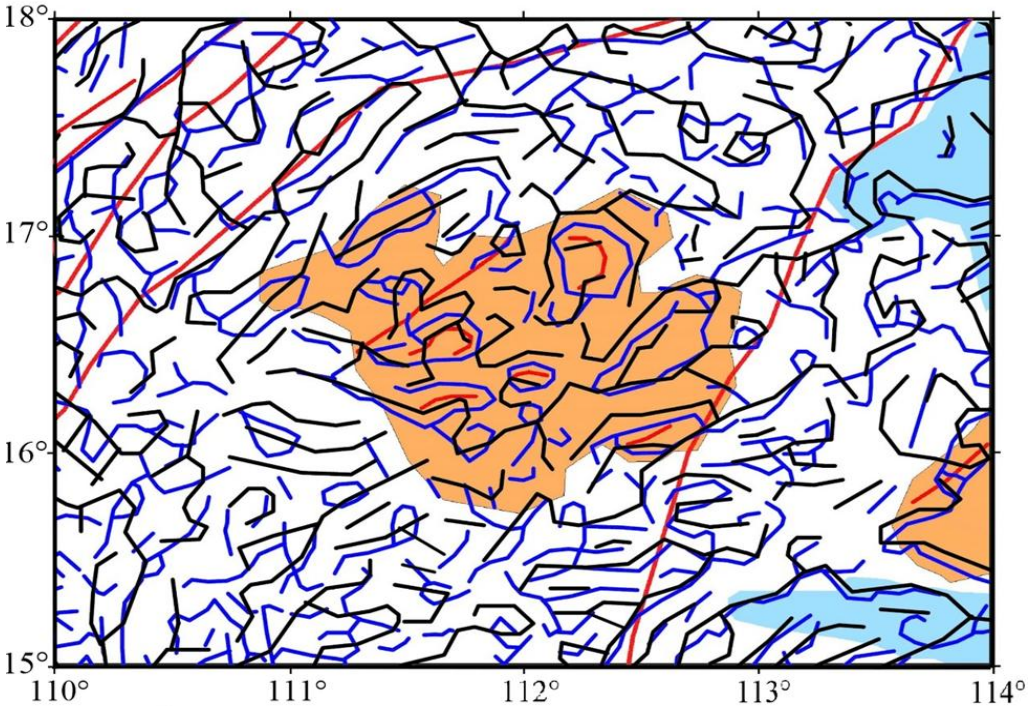

Fig. 10. Gravity (black lines) and topographic (blue lines) lineaments are overlapping on the tectonic map. The red lines show the known faults.

Conclusions

The interpretation of Bouguer gravity data of the Paracel Islands, processed using modern methods and combined with bathymetric data interpretation, allowed us to map the structures in the islands. The results showed that the EHGA and IL methods provide better results than the ETHD, ITDX, ITM, and ILTHD methods in determining the structures. The information obtained from the EHGA and IL methods is clear, precise, and high-resolution without generating second boundaries. The obtained structural map of the study region reveals that the boundaries follow the NE–SW, NW–SE, NNW–SSE, WNW–ESE, and WSW–ENE orientations. The geological characteristics in the area are ideal conditions for the formation and accumulation of petroleum. Therefore, the findings from this study could aid future research in gaining a deeper understanding of the geological structures of the islands.

Acknowledgments

Ngo Thi To Nhu was funded by the Master, PhD Scholarship Programme of Vingroup Innovation Foundation (VINIF), code VINIF.2023.ThS.101.

References

Ai, H., Deniz Toktay, H., Alvandi, A., Pašteka, R., Su, K., Liu, Q. (2024): Advancing potential field data analysis: the modified horizontal gradient amplitude method (MHGA). Contributions to Geophysics and Geodesy 54(2): 119–143. https://doi.org/10.31577/congeo.2024.54.2.1

Alvandi, A., and Ardestani, V.E. (2023): Edge detection of potential field anomalies using the Gompertz function as a high-resolution edge enhancement filter. Bulletin of Geophysics and Oceanography 64(3): 279-300. https://doi.org/10.4430/bgo00420

Alvandi, A., Su, K., Ai, H., Ardestani, V.E., and Lyu, C. (2023): Enhancement of Potential Field Source Boundaries Using the Hyperbolic Domain (Gudermannian Function). Minerals 13(10): 1312. https://doi.org/10.3390/min13101312

Chen, A.G., Zhou, T.F., Liu, D.J, Zhang, S. (2017): Application of an enhanced theta-based filter for potential field edge detection: a case study of the Luzong ore district. Chinese Journal of Geophysics 60(2): 203–218. https://doi.org/10.6038/cjg20170228

Cooper, G.R.J., Cowan, D.R. (2006): Enhancing potential field data using filters based on the local phase. Computers & Geosciences 32: 1585-1591. https://doi.org/10.1016/j.cageo.2006.02.016

Bouchat, C.J. (2014): The Paracel Islands and US interests and approaches in the South China Sea. Department of the Army.

Ekinci, Y.L, Ertekin, C., Yigitbas, E. (2013): On the effectiveness of directional derivative based filters on gravity anomalies for source edge approximation: synthetic simulations and a case study from the Aegean graben system (Western Anatolia, Turkey). Journal of Geophysics and Engineering 10(3): 035005. https://doi.org/10.1088/1742-2132/10/3/035005

Ekwok, S.E., Eldosuoky, A.M., Thompson, E.A., Ojong, R.A., George, A.M., Alarifi, S.S., Kharbish, S., Andráš, P., Akpan, A.E. (2024): Mapping of geological structures and sediment thickness from analysis of aeromagnetic data over the Obudu Basement Complex of Nigeria. Journal of Geophysics and Engineering 21(2): 413-425. https://doi.org/10.1093/jge/gxae012

Eldosouky, A.M., Pham, L.T., Duong, V.H., Ghomsi, F.E.K. and Henaish, A. (2022a): Structural interpretation of potential field data using the enhancement techniques: A case study. Geocarto International 37(27): 16900-16925. https://doi.org/10.1080/10106049.2022.2120548

Eldosouky, A.M., Pham, L.T., Henaish, H. (2022b): High precision structural mapping using edge filters of potential field and remote sensing data: A case study from Wadi Umm Ghalqa area, South Eastern Desert, Egypt. The Egyptian Journal of Remote Sensing and Space Science 25(2): 501-513. https://doi.org/10.1016/j.ejrs.2022.03.001

Ferreira, F.J.F., de Souza, J., de Bongiolo, A.B.e.S., de Castro, L.G. (2013): Enhancement of the total horizontal gradient of magnetic anomalies using the tilt angle. Geophysics 78(3): 33-41. https://doi.org/10.1190/geo2011-0441.1

Foerste, C. (2014): EIGEN-6C4: the latest combined global gravity field model including GOCE data up to degree and order 2190 of GFZ Potsdam and GRGS Toulouse. GFZ Data Services. https://doi.org/10.5880/icgem.2015.1.

Hamimi, Z., Eldosouky, A.M., Hagag, W., and Kamh, S.Z. (2023): Large-scale geological structures of the Egyptian Nubian Shield. Scientific Reports 13(1): 1923. https://doi.org/10.1038/s41598-023-29008-x

Ghomsi, F.E.K., Pham, L.T., Tenzer, R., Esteban, F.D., Vu, T.V., Kamguia, J. (2022a): Mapping of fracture zones and structural lineaments of the Gulf of Guinea passive margins using marine gravity data from CryoSat-2 and Jason-1 satellites. Geocarto International 37(25): 10819–10842. https://doi.org/10.1080/10106049.2022.2040602

Ghomsi, F.E.K., Pham, L.T., Steffen, R., Ribeiro-Filho, N., Tenzer, R. (2022b): Delineating structural features of North Cameroon using EIGEN6C4 high-resolution global gravitational model. Geological journal 57(10):4285–4299. https://doi.org/10.1002/gj.4544

Luong, L.D., Hoang, N., Shinjo, R., Shakirov, R.B., Obzhirov, A. (2021): Chemical, mineralogical, and physicochemical features of surface saline muds from Southwestern sub-basin of the East Vietnam Sea: Implication for new peloids. Vietnam Journal of Earth Sciences 43(4): 496-508, https://doi.org/10.15625/2615-9783/16561

Kafadar, O. (2017): CURVGRAV-GUI: A graphical user interface to interpret gravity data using curvature technique. Earth Science Informatics 10(4): 525–537. https://doi.org/10.1007/s12145-017-0306-6

Kafadar, O. (2022): Applications of the Kuwahara and Gaussian filters on potential field data. Journal of Applied Geophysics 198: 104583. https://doi.org/10.1016/j.jappgeo.2022.104583

Kamto, P.G., Oksum, E., Pham, L.T., Kamguia, J. (2023): Contribution of advanced edge detection filters for the structural mapping of the Douala Sedimentary Basin along the Gulf of Guinea. Vietnam Journal of Earth Sciences 45(3): 287–302. https://doi.org/10.15625/2615-9783/18410

Li, X., Shi Z., Han L., Hu, X. (2023): Geochemical characteristics of hydrogen, oxygen, carbon isotopes and REE of cenozoic dolomites in Well Xike 1, Xisha Islands, South China sea and the significance for dolomitization in islandreef areas. Front. Earth Sci. 10:1064808. https://doi.org/10.3389/feart.2022.1064808

Ma, G., Huang, D., and Liu, C. (2016): Step-Edge Detection Filters for the Interpretation of Potential Field Data. Pure and Applied Geophysics 173: 795–803. https://doi.org/10.1007/s00024-015-1053-6

Manh, H.N., and Dinh, T.H. (2014): Bien Dong seafloor spreading and its influence to formation & development of sedimentary basins. Science and Technology Development Journal, 17(3): 132-138. https://doi.org/10.32508/stdj.v17i3.1494

Melouah, O., Pham, L.T. (2021): An improved ILTHG method for edge enhancement of geological structures: application to gravity data from the Oued Righ valley. Journal of African earth sciences

177: 104162. https://doi.org/10.1016/j.jafrearsci.2021.104162
Melouah, O., Ebong, E.D., Abdelrahman, K. et al. (2023): Lithospheric structural dynamics and geothermal modeling of the Western Arabian Shield. Scientific Reports 13:11764. https://doi.org/10.1038/s41598-023-38321-4
Nasuti, Y., Nasuti, A. (2018): NTilt as an improved enhanced tilt derivative filter for edge detection of potential field anomalies. Geophysical Journal International 214(1): 36–45. https://doi.org/10.1093/gji/ggy117
Nasuti, Y., Nasuti, A., Moghadas, D. (2019): STDR: a novel approach for enhancing and edge detection of potential field data. Pure and Applied Geophysics 176: 827–841. https://doi.org/10.1007/s00024-018-2016-5
Nzeuga, A.R., Ghomsi, F.E., Pham, L.T., Eldosouky, A.M., et al. (2022): Contribution of advanced edge detection methods of potential field data in the tectono-structural study of the southwestern part of Cameroon. Frontiers in Earth Science 10: 970614. https://doi.org/10.3389/feart.2022.970614
Nhu, H.T., Nguyen, B.K., Van, X.T., Xuan, K.N., Xuan, H.N., and Van, T.N. (2014): The tectonic evolution and hydrocarbon potential in the boundaries of Vietnam continental shelf. Science and Technology Development Journal 17(3): 126-131. https://doi.org/10.32508/stdj.v17i3.1490
Oksum, E., Le, D.V., Vu, M.D., Nguyen, T.H.T., Pham, L.T. (2021): A novel approach based on the fast sigmoid function for interpretation of potential field data. Bulletin of Geophysics and Oceanography 62(3): 543–556. https://doi.org/10.4430/bgta0348
Pal, S.K., Narayan, S., Majumdar, T.J., Kumar, U. (2016): Structural mapping over the 85° E Ridge and surroundings using EIGEN6C4 high-resolution global combined gravity field model: an integrated approach. Marine Geophysical Research 37: 159–184. https://doi.org/10.1007/s11001-016-9274-3.
Pham, H.T., et al. (2023): Performance evaluation of high/ultra-high-degree global geopotential models over Vietnam using GNSS/leveling data. Geodesy and Geodynamics 14(5): 500-512. https://doi.org/10.1016/j.geog.2023.03.002
Pham, L.T. (2023): A novel approach for enhancing potential fields: application to aeromagnetic data of the Tuangiao, Vietnam. The European Physical Journal Plus 138(12): 1-11. https://doi.org/10.1140/epjp/s13360-023-04760-1
Pham, L.T. (2024a): A stable method for detecting the edges of potential field sources. IEEE Transactions on Geoscience and Remote Sensing 62: 5912107. https://doi.org/10.1109/TGRS.2024.3388294
Pham, L.T. (2024b): Mapping the structural configuration of the northern part of the Central Indian Ridge from satellite gravity data using derivatives of the horizontal gradient. Advances in Space Research. https://doi.org/10.1016/j.asr.2024.05.054
Pham, L.T. (2024c): An improved edge detector for interpreting potential field data. Earth Science Informatics 17(3) 2763–2774. https://doi.org/10.1007/s12145-024-01286-7
Pham, L.T. (2024d): A new technique based on the eigenvalue of the curvature tensor for enhancing gravity data", Annals of Geophysics 67(2) DM213. https://doi.org/10.4401/ag-9050.
Pham, L.T., Oksum, E., Do, T.D., & Huy, M.L. (2018) New method for edges detection of magnetic sources using logistic function. Geofizicheskiy Zhurnal 40(6): 127–135. https://doi.org/10.24028/gzh.0203-3100.v40i6.2018.151033
Pham, L.T., Eldosouky, A.M., Oksum, E., Saada, S.A. (2020a): A new high resolution filter for source edge detection of potential field data. Geocarto International 37(11): 3051-3068. https://doi.org/10.1080/10106049.2020.1849414
Pham, L.T., Van Vu, T., Le Thi, S., Trinh, P.T. (2020b): Enhancement of potential field source boundaries using an improved logistic filter. Pure and Applied Geophysics 177: 5237-5249. https://doi.org/ 10.1007/s00024-020-02542-9.
Pham, L.T., Oksum, E., Kafadar, O., Trinh, P.T., Nguyen, D.V., Vo, Q.T., Le, S.T. (2022a): Determination of subsurface lineaments in the Hoang Sa islands using enhanced methods of gravity total horizontal gradient. Vietnam Journal of Earth Science 44(3): 395-409. https://doi.org/10.15625/2615-9783/17013.
Pham, L.T., Nguyen, T.X., Eldosouky, A.M., Do, T.D., & Nguyen, T.Q. (2022b): The utility of the enhancement techniques for mapping subsurface structures from gravity data. Frontiers in Scientific Research and Technology 3(1): 11-19. https://doi.org/10.21608/fsrt.2021.94294.1047
Pham, L.T., Oliveira, S.P., Le Huy, M., Nguyen, D.V, Nguyen Dang, T.Q., Do, T.D., Tran, K.V., Nguyen, H.D.T., Ngo, T.N.T., Pham, H.Q. (2024a): Reliable Euler deconvolution solutions of gravity data throughout the β-VDR and THGED methods: Application to mineral exploration and geological structural mapping. Vietnam Journal of Earth Sciences 46(3): 432–448. https://doi.org/10.15625/2615-9783/21009
Pham, L.T., Abdelrahman, K., Nguyen, D.V., Gomez Ortiz, D., Long, N.N., Luu, L.D., Do, T.D., Vo, Q.T., Nguyen, T.T.T., Nguyen, H.D.T., Eldosouky, A.M. (2024b): Enhancement of the balanced total horizontal derivative of gravity data using the power law approach. Geocarto International 39(1): 2335251. https://doi.org/10.1080/10106049.2024.2335251
Pham, L.T., Prasad, K.N.D. (2023): Analysis of gravity data for extracting structural features of the northern region of the Central Indian Ridge. Vietnam Journal of Earth Sciences 45(2): 147–163. https://doi.org/10.15625/2615-9783/18206
Pham, L.T., Prasad, K.N.D. (2024): Gravity patterns and crustal architecture of the South-Central Indian Ridge at 22°-17°S: Evidence for the asymmetric ridge accretion. Journal of Asian Earth Sciences 260: 105966. https://doi.org/10.1016/j.jseaes.2023.105966
Prasad, K.N.D., Pham, L.T., Singh, A.P. (2022a): Structural mapping of potential field sources using BHG filter. Geocarto International 37(26): 11253-11280. https://doi.org/10.1080/10106049.2022.2048903
Prasad, K.N.D., Pham, L.T., Singh, A.P. (2022b): A novel filter "ImpTAHG" for edge detection and a case study from Cambay Rift Basin, India. Pure and Applied Geophysics 179(6): 2351–2364. https://doi.org/10.1007/s00024-022-03059-z
Prasad, K.N.D., Pham, L.T., Singh, A.P., Eldosouky, A.M., Abdelrahman, K., Fnais, M.S., Gómez-Ortiz D (2022c): A novel enhanced total gradient (ETG) for interpretation of magnetic data. Minerals 12(11):1468. https://doi.org/10.3390/min12111468
Roy, P., Sai Krishnaveni, A., Vinod Kumar, K. Geological evaluation of EIGEN-6C4 and GOCE derived gravity models in and around Karakoram shear zone, Leh, India. J Geol Soc India 90, 51–61 (2017). https://doi.org/10.1007/s12594-017-0663-2
Saada, A.S., Eldosouky, A.M., Abdelrahman, K., Al Otaibi, N., Ibrahim, E., Ibrahim, A. (2021): New insights into the contribution of gravity data for mapping the lithospheric architecture. Journal of King Saud University - Science 33(3): 101400. https://doi.org/10.1016/j.jksus.2021.101400
Saada, S.A., Eldosouky, A.M., Kamel, M., El Khadragy, A., Abdelrahman, K., Fnais, M.S., Mickus, K. (2022): Understanding the structural framework controlling the sedimentary basins from the integration of gravity and magnetic data: A case study from the east of the Qattara Depression area, Egypt. Journal of King Saud University – Science 34(2): 101808. https://doi.org/10.1016/j.jksus.2021.101808
Sahoo, S., Narayan, S., Pal, S.K. (2022a): Fractal analysis of lineaments using CryoSat-2 and Jason-1 satellite derived gravity data: evidence of a uniform tectonic activity over the middle part of the Central Indian Ridge. Physics and Chemistry of the Earth 128: 103237. https://doi.org/10.1016/j.pce.2022.103237
Sahoo, S., Narayan, S., Pal, S.K. (2022b): Appraisal of gravity-

based lineaments around Central Indian Ridge (CIR) in different geological periods: evidence of frequent ridge jumps in the southern block of CIR. Journal of Asian Earth Sciences 239: 105393. https://doi.org/10.1016/j.jseaes.2022.105393

Sahoo, S.D., Pal, S.K. (2019): Mapping of Structural Lineaments and Fracture Zones around the Central Indian Ridge (10◦S–21◦S) using EIGEN 6C4 Bouguer Gravity Data. Journal of the Geological Society of India 94(4): 359–366. https://doi.org/10.1007/s12594-019-1323-5

Pham, L.T., Prasad, K.N.D. (2023): Analysis of gravity data for extracting structural features of the northern region of the Central Indian Ridge. Vietnam Journal of Earth Sciences 45(2): 147–163. https://doi.org/10.15625/2615-9783/18206

Sibuet, J.C., Yeh, Y.C., and Lee, C.S. (2016): Geodynamics of the South China Sea. Tectonophysics 692: 98-119. https://doi.org/10.1016/j.tecto.2016.02.022

Steffen, R., Strykowski, G., and Lund, B. (2017): High-resolution Moho model for Greenland from EIGEN-6C4 gravity data. Tectonophysics 706: 206-22. https://doi.org/10.1016/j.tecto.2017.04.014

Wijns, C., Perez, C., Kowalczyk, P. (2005): Theta map: Edge detection in magnetic data. Geophysics 70: 39-43. https://doi.org/10.1190/1.1988184

Yang, Z., Zhang, G., Wu, S., Zhu, Y., Wu, C., Zhang, L., Liu, S., Yan, W., Sun, M., Zhang, Y., et al. (2022): Geological Distribution of the Miocene Carbonate Platform in the Xisha Sea Area of the South China Sea, and Its Implications for Hydrocarbon Exploration. Applied Sciences 12: 11831. https://doi.org/ 10.3390/app122211831